Hindawi Publishing Corporation
Shock and Vibration
Volume 2015, Article ID 183756, 15 pages
http://dx.doi.org/10.1155/2015/183756

Research Article

Seismic Response Analysis of Continuous Multispan Bridges with Partial Isolation

E. Tubaldi,[1] A. Dall'Asta,[2] and L. Dezi[1]

[1]*Department of Construction, Civil Engineering and Architecture (DICEA), Polytechnic University of Marche, Via Brecce Bianche, 60131 Ancona, Italy*
[2]*School of Architecture and Design (SAD), University of Camerino, Viale della Rimembranza, 63100 Ascoli Piceno, Italy*

Correspondence should be addressed to E. Tubaldi; etubaldi@gmail.com

Received 17 December 2014; Accepted 23 March 2015

Academic Editor: Laurent Mevel

Partially isolated bridges are a particular class of bridges in which isolation bearings are placed only between the piers top and the deck whereas seismic stoppers restrain the transverse motion of the deck at the abutments. This paper proposes an analytical formulation for the seismic analysis of these bridges, modelled as beams with intermediate viscoelastic restraints whose properties describe the pier-isolator behaviour. Different techniques are developed for solving the seismic problem. The first technique employs the complex mode superposition method and provides an exact benchmark solution to the problem at hand. The two other simplified techniques are based on an approximation of the displacement field and are useful for preliminary assessment and design purposes. A realistic bridge is considered as case study and its seismic response under a set of ground motion records is analyzed. First, the complex mode superposition method is applied to study the characteristic features of the dynamic and seismic response of the system. A parametric analysis is carried out to evaluate the influence of support stiffness and damping on the seismic performance. Then, a comparison is made between the exact solution and the approximate solutions in order to evaluate the accuracy and suitability of the simplified analysis techniques for evaluating the seismic response of partially isolated bridges.

1. Introduction

Partially restrained seismically isolated bridges (PRSI) are a particular class of bridges isolated at intermediate supports and transversally restrained at abutments. This type of partial isolation is quite common in many bridges all over the world (see, e.g., [1–4]). The growing interest on the dynamic behaviour of bridges with partial restrain is demonstrated by numerous recent experimental works [3, 4] and numerical studies [5–11] discussing the advantages and drawbacks with respect to full isolation.

An analytical model commonly employed for the analysis of the transverse behaviour of PRSI bridges consists in a continuous simply supported beam resting on discrete intermediate supports with viscoelastic behaviour representing the pier-bearing systems (see, e.g., [6, 8, 9]). The damping is promoted by two different mechanisms: the bearings, usually characterized by high dissipation capacity, and the deck, characterized by a lower but widespread dissipation capacity. The strongly inhomogeneous distribution of the dissipation properties along the bridge results in nonclassical damping and this makes the rigorous analysis of the analytical PRSI bridge model very demanding.

In general, the exact solution of the seismic problem for a nonclassically damped system requires resorting to the direct integration of the equations of motion or to modal analysis [12] based on complex vibration modes. The first analysis approach is conceptually simple, though computationally costly when large-scale systems are analyzed, whereas the second approach is computationally efficient but often not appealing for practical engineering applications since it involves complex-valued functions and it is difficult to implement in commercial finite element codes. For this reason, many studies have been devoted to the definition of approximate techniques of analysis and to the assessment of their accuracy [13–17]. With reference to the classical case of fully isolated bridges, the studies of Hwang et al. [18] and Lee et al. [19] have shown that acceptable estimates

of the modal damping ratios are obtained by considering the real undamped modes and the diagonal terms of the modal damping matrix. Franchin et al. [20] have analyzed some realistic bridge models by showing that this decoupling approximation gives also quite accurate estimates of the response to a seismic input, as compared to the rigorous response estimates obtained through complex modal analysis. With reference to the specific case of PRSI bridges, characterized by deformation shapes and dynamic properties very different from those of fully isolated bridges, the work of Tubaldi and Dall'Asta [9] has addressed the issue of nonclassical damping within the context of the free-vibration response. The authors have observed that nonclassical damping influences differently the various response parameters relevant for the performance assessment (i.e., the transverse displacement shape is less affected than the bending moment demand by the damping nonproportionality). However, the effects of the decoupling approximation on the evaluation of the seismic response of the proposed PRSI bridge model have not been investigated yet. This issue becomes of particular relevance in consequence of the numerous studies on PRSI bridges that completely disregard nonclassical damping [6–8]. Thus, a closer examination is still required to ensure whether the use of proportionally damped models provides acceptable estimates of the seismic response of these systems.

Another approximation often introduced in the analysis of PRSI bridges concerns the transverse deformation shape. In this regard, many studies are based on the assumption of a prefixed sinusoidal vibration shape [6, 8, 10]. This assumption permits deriving analytically the properties of a generalized SDOF system equivalent to the bridge and estimating the system response by expressing the seismic demand in terms of a response spectrum reduced to account for the system composite damping ratio. In Tubaldi and Dall'Asta [8, 9], it is shown that the sinusoidal approximation of the transverse displacements may be accurate for PRSI bridges if the following conditions are met: (a) the superstructure stiffness is significantly higher than the pier stiffness, (b) the variations of mass and stiffness of the deck and of the supports are not significant, (c) the span number is high, and (d) the displacement field is dominated by the first vibration mode. However, even if the displacements are well described by a sinusoidal shape, other response parameters of interest for the performance assessment such as the transverse bending moments may not exhibit a sinusoidal shape. Thus, further investigations are required to estimate the error arising due to this approximation.

The aim of this study is to develop an analytical formulation of the seismic problem of PRSI bridges, modelled as nonclassically damped continuous systems, and a rigorous solution technique based on the complex mode superposition (CMS) method [12, 21–24]. The application of this method requires the derivation of the expression of the modal orthogonality conditions and of the impulsive response specific to the problem at hand. It permits describing the seismic response in terms of superposition of the complex vibration modes, which is particularly useful for this case in consequence of the relevant contribution of higher modes of vibration to the response of PRSI bridges [8, 10]. Moreover, the proposed technique permits testing the accuracy of two simplified analysis techniques introduced in this study and commonly employed for the PRSI bridge analysis. The first approximate technique describes the transverse motion through a series expansion in terms of the classic modes of vibration, obtained by neglecting the damping of the intermediate restraints, whereas the second technique is based on a series expansion in terms of sinusoidal functions, corresponding to the vibration modes of the system without the intermediate restraints. The introduction of these approximations of the displacement field results in a coupling of the equation of motions projected in the space of the approximating functions, which is neglected in the solution to simplify the response assessment.

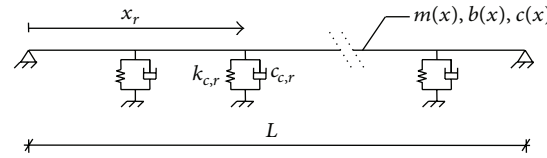

Figure 1: Analytical model for PRSI bridges.

A realistic case study is considered and its response to a set of ground motion records is examined first through the CMS method with these two objectives: to unveil the characteristic features of the performance of PRSI bridges and to assess the influence of higher vibration modes and of the intermediate support stiffness and damping on the response of the resisting components. Successively, the seismic response estimates according to the CMS method are compared with the corresponding estimates obtained by applying the proposed simplified techniques, in order to evaluate their accuracy and reliability.

2. Dynamic Behavior of PRSI Bridges

The PRSI bridge model (Figure 1) consists of beam pinned at the abutments and resting on discrete viscoelastic supports representing the pier-bearing systems.

Let $H^2[\Omega]$ be the space of functions with square integrable second derivatives in the spatial interval $\Omega = [0, L]$, V the space of transverse displacement functions satisfying the kinematic boundary conditions (e.g., $V = \{v(x) \in H^2[\Omega] : v(0) = v(L) = 0\}$), and $u(x,t) \in U \subseteq C^2(V; [t_0, t_1])$ the motion, defined in the time interval considered $[t_0, t_1]$, belonging to the space of continuous functions C^2 and known at the initial instant together with its time derivative (initial conditions). The differential dynamic problem can be derived from the D'Alembert principle [25] and expressed in the following form:

$$\int_0^L m(x)\,\ddot{u}(x,t)\,\eta(x)\,dx + \int_0^L c(x)\,\dot{u}(x,t)\,\eta(x)\,dx + \sum_{r=1}^{N_c} c_{c,r}\dot{u}(x_r,t)\,\eta(x_r) + \int_0^L b(x)\,u''(x,t)\,\eta''(x)\,dx$$

$$+\sum_{r=1}^{N_c} k_{c,r} u(x_r,t)\,\eta(x_r) = -\int_0^L m(x)\,\ddot{u}_g(t)\,\eta(x)\,dx \qquad \forall \eta \in V; \quad \forall t \in [t_0,t_1], \tag{1}$$

where $\eta \in V$ denotes a virtual displacement consistent with the geometric restrains, N_c denotes the number of intermediate supports, prime denotes differentiation with respect to x and dot differentiation with respect to time t.

The piecewise continuous functions $m(x)$, $b(x)$, and $c(x)$ denote the mass per unit length, the transverse bending stiffness per unit length, and the deck distributed damping constant. The constants $k_{c,r}$ and $c_{c,r}$ are the stiffness and damping constant of the viscoelastic support located at the rth position $= x_r$, while $\ddot{u}_g(t)$ denotes the ground acceleration.

The local form of the problem is obtained by integrating by parts (1) and can be formally written as

$$M\ddot{u}(x,t) + C\dot{u}(x,t) + Ku(x,t) = -M\ddot{u}_g(t), \qquad u'''(x,t)\,\eta\big|_0^L = 0, \qquad u''(x,t)\,\eta'\big|_0^L = 0, \tag{2}$$

where M, C, and K denote, respectively, the mass, damping, and stiffness operator. They are expressed as (δ is the Dirac's delta function)

$$M = m(x)$$
$$K = b(x)\frac{\partial^4}{\partial x^4} + \sum_{r=1}^{N_c} k_{c,r}\delta(x-x_r) \tag{3}$$
$$C = c(x) + \sum_{r=1}^{N_c} c_{c,r}\delta(x-x_r).$$

3. Eigenvalue Problem for PRSI Bridges

The free-vibrations problem of the beam is obtained by posing $\ddot{u}_g = 0$ in (2). The corresponding differential boundary problem is then reduced to an eigenvalue problem solvable by expressing the transverse displacement $u(x,t)$ as the product of a spatial function $\psi(x)$ and a time-dependent function $Z(t) = Z_0 e^{\lambda t}$:

$$u(x,t) = \psi(x)\,Z(t). \tag{4}$$

After substituting (3) and (4) into (2) for $\ddot{u}_g = 0$, the following transcendental equation is obtained:

$$\left[m(x)\lambda^2 + c(x)\lambda\right]\psi(x) + b(x)\psi^{IV}(x) + \sum_{r=1}^{N_c}\left(k_{c,r} + c_{c,r}\lambda\right)\delta(x-x_r)\,\psi(x) = 0. \tag{5}$$

Equation (5) is satisfied by an infinite number of eigenvalues and eigenvectors that occur in complex conjugate pairs [26]. The ith eigenvalue λ_i contains information about the system vibration frequency and damping, while the ith eigenvector $\psi_i(x)$ is the ith vibration shape. The solution of the eigenvalue problem for constant deck properties is briefly recalled in the appendix. The orthogonality conditions for the complex modes are [9]

$$\left(\lambda_i + \lambda_j\right)\int_0^L m(x)\,\psi_i(x)\,\psi_j(x)\,dx + \int_0^L c(x)\,\psi_i(x)\,\psi_j(x)\,dx + \sum_{r=1}^{N_c} c_{c,r}\psi_i(x_r)\,\psi_j(x_r) = 0 \tag{6}$$

$$\int_0^L b(x)\,\psi_i''(x)\,\psi_j''(x)\,dx - \lambda_i\lambda_j\int_0^L m(x)\,\psi_i(x)\,\psi_j(x)\,dx + \sum_{r=1}^{N_c} k_{c,r}\psi_i(x_{c,r})\,\psi_j(x_{c,r}) = 0. \tag{7}$$

4. Seismic Response of PRSI Bridges Based on CMS Method

4.1. Series Expansion of the Response. In the CMS method, the displacement of the beam is expanded as a series of the complex vibration modes as

$$u(x,t) = \sum_{i=1}^{\infty}\psi_i(x)\,q_i(t), \tag{8}$$

where $\psi_i(x) = i$th complex modal shape and $q_i(t) = i$th complex generalized coordinate. It is noteworthy that, in practical applications, the series is truncated at the term N_m.

Substituting (8) into (1) written for $\eta(x) = \psi_j(x)$ one obtains

$$\sum_{i=1}^{\infty}\left[\int_0^L m(x)\,\psi_i(x)\,\psi_j(x)\,dx\right]\ddot{q}_i(t) + \sum_{i=1}^{\infty}\left[\int_0^L c(x)\,\psi_i(x)\,\psi_j(x)\,dx + \sum_{r=1}^{N_c} c_{c,r}\psi_i(x_{c,r})\,\psi_j(x_{c,r})\right]\dot{q}_i(t) + \sum_{i=1}^{\infty}\left[\int_0^L b(x)\,\psi_i''(x)\,\psi_j''(x)\,dx + \sum_{r=1}^{N_c} k_{c,r}\psi_i(x_{c,r})\,\psi_j(x_{c,r})\right]q_i(t) = -\int_0^L m(x)\,\psi_j(x)\,\ddot{u}_g(t)\,dx. \tag{9}$$

Upon substitution of (7) into (9) the following expression is obtained

$$\begin{aligned}&\sum_{i=1}^{\infty}\ddot{q}_i(t)\left[\int_0^L m(x)\,\psi_i(x)\,\psi_j(x)\,dx\right]\\&\quad+\sum_{i=1}^{\infty}\dot{q}_i(t)\left[\int_0^L c(x)\,\psi_i(x)\,\psi_j(x)\,dx\right.\\&\qquad\left.+\sum_{r=1}^{N_c}c_{c,r}\psi_i\left(x_{c,r}\right)\psi_j\left(x_{c,r}\right)\right]\\&\quad+\sum_{i=1}^{\infty}q_i(t)\left[\lambda_i\lambda_j\int_0^L m(x)\,\psi_i(x)\,\psi_j(x)\,dx\right]\\&=-\int_0^L m(x)\,\psi_j(x)\,\ddot{u}_g(t)\,dx.\end{aligned}\tag{10}$$

4.2. Response to Impulsive Loading. For $\ddot{u}_g(t) = \delta(t)$, the generalized coordinate assumes the form [22]

$$q_i(t) = B_i e^{\lambda_i t}\tag{11}$$

with $\dot{q}_i(t) = \lambda_i q_i(t)$ and $\ddot{q}_i(t) = {\lambda_i}^2 q_i(t)$.

After substituting into (10), one obtains

$$\begin{aligned}&\sum_{i=1}^{\infty}\frac{\ddot{q}_i(t)}{\lambda_i}\left[\left(\lambda_i+\lambda_j\right)\int_0^L m(x)\,\psi_i(x)\,\psi_j(x)\,dx\right.\\&\qquad+\int_0^L c(x)\,\psi_i(x)\,\psi_j(x)\,dx\\&\qquad\left.+\sum_{r=1}^{N_c}c_{c,r}\psi_i\left(x_{c,r}\right)\psi_j\left(x_{c,r}\right)\right]\\&=-\delta(t)\int_0^L m(x)\,\psi_j(x)\,dx.\end{aligned}\tag{12}$$

It can be noted that the right-hand side of (12) vanishes for $\lambda_i \neq \lambda_j$ by virtue of (6). Thus, the problem can be diagonalized and the ith decoupled equation reads as follows:

$$2\widehat{M}_i\ddot{q}_i(t) + \widehat{C}_i\dot{q}_i(t) = -\widehat{L}_i\delta(t),\tag{13}$$

where $\widehat{M}_i = \int_0^L m(x){\psi_i}^2(x)dx$, $\widehat{C}_i = \int_0^L c(x){\psi_i}^2(x)dx + \sum_{r=1}^{N_c} c_{c,r}{\psi_i}^2(x_{c,r})$, and $\widehat{L}_i = \int_0^L m(x)\psi_i(x)dx$.

By assuming that the system is at rest for $t < 0$, the following equation holds at $t = 0^+$:

$$2\widehat{M}_i\dot{q}_i\left(0^+\right) + \widehat{C}_i q_i\left(0^+\right) = -\widehat{L}_i.\tag{14}$$

Thus, since $q_i(0^+) = B_i$ and $\dot{q}_i(0^+) = \lambda B_i$, one can finally express B_i as

$$\begin{aligned}B_i &= \frac{\widehat{L}_i}{2\widehat{M}_i\lambda_i + \widehat{C}_i}\\&= -\left(\int_0^L m(x)\,\psi_i(x)\,dx\right)\\&\quad\cdot\left(2\lambda_i\int_0^L m(x)\,{\psi_i}^2(x)\,dx + \int_0^L c(x)\,{\psi_i}^2(x)\,dx\right.\\&\qquad\left.+\sum_{r=1}^{N_c}c_{c,r}{\psi_i}^2\left(x_{c,r}\right)\right)^{-1}.\end{aligned}\tag{15}$$

The corresponding expression of the complex modal impulse response function is ${h_i}^c(x,t) = B_i\psi_i(x)e^{\lambda_i t}$ and the sum of the contribution to the complex modal impulse response function of the ith mode and of its complex conjugate yields a real function $h_i(x,t)$, which may be expressed as

$$\begin{aligned}h_i(x,t) &= B_i\psi_i(x)\,e^{\lambda_i t} + \overline{B}_i\overline{\psi}_i(x)\,e^{\overline{\lambda}_i t}\\&= \alpha_i(x)\left|\lambda_i\right|h_i(t) + \beta_i(x)\,\dot{h}_i(t),\end{aligned}\tag{16}$$

where $\alpha_i(x) = \xi_i\beta_i(x) - \sqrt{1-{\xi_i}^2}\gamma_i(x)$, $\beta_i(x) = 2\,\mathrm{Re}[B_i\psi_i]$, $\gamma_i(x) = 2\,\mathrm{Im}[B_i\psi_i]$, and $h_i(t)$ denotes the impulse response function of a SDOF system with natural frequency $\omega_{0i} = |\lambda_i|$, damping ratio $\xi_i = -\mathrm{Re}(\lambda_i)/|\lambda_i|$, and damped frequency $\omega_{di} = \omega_{0i}\sqrt{1-{\xi_i}^2}$, whose expression is

$$h_i(t) = \frac{1}{\omega_{di}}e^{-\xi_i\omega_{0i}t}\sin\left(\omega_{di}t\right).\tag{17}$$

4.3. CMS Method for Seismic Response Assessment. By taking advantage of the derived closed-form expression of the impulse response function, the seismic input $\ddot{u}_g(t)$ is expressed as a sum of Delta Dirac functions as follows:

$$\ddot{u}_g(t) = \int_0^t \ddot{u}_g(\tau)\,\delta(t-\tau)\,d\tau.\tag{18}$$

The seismic displacement response is then expressed in terms of superposition of modal impulse responses:

$$\begin{aligned}u(x,t) &= \sum_{i=1}^{\infty}\int_0^t \ddot{u}_g(\tau)\,h_i(x,t-\tau)\,d\tau\\&= \sum_{i=1}^{N_m}\alpha_i(x)\left|\lambda_i\right|D_i(t) + \beta_i(x)\,\dot{D}_i(t),\end{aligned}\tag{19}$$

where $D_i(t)$ and $\dot{D}_i(t)$ denote the response of the oscillator with natural frequency ω_{0i} and damping ratio ξ_i, subjected to the seismic input $\ddot{u}_g(t)$.

It is noteworthy that in the case of $c_{c,r} = 0$, corresponding to intermediate supports with no damping, the system

becomes classically damped and one obtains $\lambda_i = -\xi_i\omega_{0i} + i\omega_{0i}\sqrt{1-\xi_i^2}$, $\xi_i = c_d/(2\omega_{0i}m_d)$, $B_i = -\rho_i i/(2\omega_{0i}\sqrt{1-\xi_i^2})$, $\alpha_i = \rho_i/\omega_{0i}$, $\beta_i = 0$, and $\gamma_i = -\rho_i/(\omega_{0i}\sqrt{1-\xi_i^2})$, where $\rho_i = i$th is the real mode participation factor. Thus (19) reduces to the well-known expression:

$$u(x,t) = \sum_{i=1}^{\infty} \rho_i D_i(t). \tag{20}$$

The expression of the other quantities that can be of interest for the seismic performance assessment of PRSI bridges can be derived by differentiating (19). In particular, the abutment reactions are obtained as $R_{ab}(0,t) = -b(0)u'''(0,t)$ and $R_{ab}(L,t) = -b(L)u'''(L,t)$, the rth pier reaction is obtained as $R_{pr} = k_{c,r}u(x_r,t) + c_{c,r}\dot{u}(x_r,t)$ for $r = 1,2,\ldots,N_c$, and the transverse bending moments are obtained as $M(x,t) = -b(x)u''(x,t)$.

5. Simplified Methods for Seismic Response Assessment

In this paragraph, two simplified approaches often employed for the seismic analysis of structural systems are introduced and discussed. These approaches are both based on the assumed modes method [27, 28] and entail using in (8) a complete set of approximating real-valued functions (denoted as $\eta_i(x)$ for $i = 1,2,\ldots,\infty$) instead of the exact complex vibration modes for describing the displacement field. The two analysis techniques differ for the approximating function employed. The use of these functions leads to a system of coupled Galerkin equations [27], and the generic ith equation reads as follows:

$$\sum_{j=1}^{\infty} M_{ij}\ddot{q}_j(t) + \sum_{j=1}^{\infty}\left(C_{c,ij} + C_{d,ij}\right)\dot{q}_j(t) + \sum_{j=1}^{\infty}\left(K_{c,ij} + K_{d,ij}\right)q_j(t) = -M_{p,i}\ddot{u}_g(t), \tag{21}$$

where

$$M_{ij} = \int_0^L m(x)\eta_i(x)\eta_j(x)\,dx,$$

$$M_{p,i} = \int_0^L m(x)\eta_i(x)\,dx,$$

$$K_{c,ij} = \sum_{r=1}^{N_c} k_{c,r}\eta_i(x_r)\eta_j(x_r),$$

$$K_{d,ij} = \int_0^L b(x)\eta_i''(x)\eta_j''(x)\,dx,$$

$$C_{c,ij} = \sum_{r=1}^{N_c} c_{c,r}\eta_i(x_r)\eta_j(x_r),$$

$$C_{d,ij} = \int_0^L c(x)\eta_i(x)\eta_j(x)\,dx \qquad i,j = 1,2,\ldots,\infty. \tag{22}$$

The coupling between the generalized responses $q_i(x)$ and $q_j(x)$ may be due to nonzero values of the "nondiagonal" damping and stiffness terms $C_{c,ij}$ and $K_{c,ij}$, for $i \neq j$. In order to evaluate the extent of coupling due to damping, the index α_{ij} is introduced, whose definition is [13]

$$\alpha_{ij} = \frac{\left(C_{c,ij} + C_{d,ij}\right)^2}{\left[C_{c,ii} + C_{d,ii}\right]\cdot\left[C_{c,jj} + C_{d,jj}\right]} = \left(\sum_{r=1}^{N_c} c_{c,r}\eta_i(x_r)\eta_j(x_r) + \int_0^L c_d(x)\eta_i(x)\eta_j(x)\,dx\right)^2 \cdot\left(\left(\sum_{r=1}^{N_c} c_{c,r}\eta_i^2(x_r) + \int_0^L c(x)\eta_i^2(x)\,dx\right)\cdot\left(\sum_{r=1}^{N_c} c_{c,r}\eta_j^2(x_r) + \int_0^L c(x)\eta_j^2(x)\,dx\right)\right)^{-1}. \tag{23}$$

This index assumes high values for intermediate supports with high dissipation capacity, while in the case of deck and supports with homogeneous properties it assumes lower and lower values for increasing number of supports, since the behaviour tends to that of a beam on continuous viscoelastic restraints [9].

A second coupling index is defined for the stiffness term, whose expression is

$$\beta_{ij} = \frac{\left(K_{c,ij} + K_{d,ij}\right)^2}{\left[K_{c,ii} + K_{d,ii}\right]\cdot\left[K_{c,jj} + K_{d,jj}\right]} = \left(\sum_{r=1}^{N_c} k_{c,r}\varphi_i(x_r)\varphi_j(x_r) + \int_0^L b(x)\varphi_i''(x)\varphi_j''(x)\,dx\right)^2 \cdot\left(\left(\int_0^L b(x)\left[\varphi_i''(x)\right]^2 dx + \sum_{r=1}^{N} k_{c,r}\varphi_i^2(x_r)\right)\cdot\left(\sum_{r=1}^{N_c} k_{c,r}\varphi_j^2(x_r) + \int_0^L b(x)\left[\varphi_j''(x)\right]^2 dx\right)\right)^{-1}. \tag{24}$$

It is noteworthy that β_{ij} assumes high values in the case of intermediate supports with a relatively high stiffness compared to the deck stiffness. Conversely, it assumes lower and lower values for homogenous deck and support properties and increasing number of spans, since the behaviour tends to that of a beam on continuous elastic restraints, for which $\beta_{ij} = 0$.

An approximation often introduced for practical purposes [13, 16] is to disregard the off-diagonal coupling terms

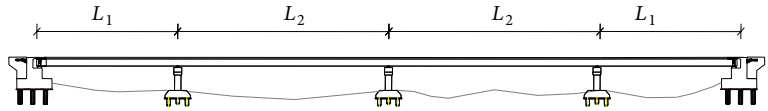

Figure 2: Bridge longitudinal profile.

to obtain a set of uncoupled equations. The resulting ith equation describes the motion of a SDOF system with mass M_{ii}, stiffness $K_{c,ii} + K_{d,ii}$, and damping constant $C_{c,ii} + C_{d,ii}$. Thus, traditional analysis tools available for the seismic analysis of SDOF systems can be employed to compute efficiently the generalized displacements $q_i(t)$ and the response $u(x,t)$, under the given ground motion excitation.

5.1. RMS Method for Seismic Response Assessment. This method, referred to as real modes superposition (RMS) method, is based on a series expansion of the displacement field in terms of the real modes of vibration $\phi_i(x)$ for $i = 1, 2, \ldots, N_m$ of the undamped (or classically damped) structure. The calculation of these classic modes of vibration involves solving an eigenvalue problem less computationally demanding than that required for computing the complex modes.

It is noteworthy that the real modes of vibration are retrieved from the PRSI bridge model of Figure 1 by neglecting the damping of the intermediate supports and that the orthogonality conditions for these modes can be obtained from (6) and (7) by posing $c_d(x) = 0$ and $c_{c,r} = 0$, for $r = 1, 2, \ldots, N_c$, leading to

$$\int_0^L m(x)\,\psi_i(x)\,\psi_j(x)\,dx = 0$$

$$\int_0^L b(x)\,\psi_i''(x)\,\psi_j''(x)\,dx + \sum_{r=1}^{N_c} k_{c,r}\psi_i(x_{c,r})\,\psi_j(x_{c,r}) = 0. \tag{25}$$

The same expressions are obtained also in the case of mass proportional damping for the deck, that is, for $c_d(x) = \kappa m(x)$ where κ is a proportionality constant.

The orthogonality conditions of (25) result in nonzero values of $C_{c,ij}$ and zero values of $K_{c,ij}$. These terms are discarded to obtain a diagonal problem.

5.2. FTS Method for Seismic Response Assessment. In the second method, referred to as Fourier terms superposition (FTS) method, the Fourier sine-only series terms $\varphi_i(x) = \sin(i\pi x/L)$ for $i = 1, 2, \ldots, N_m$ are employed to describe the motion. This method is employed in [8, 10] for the design of PRSI bridges and is characterized by a very reduced computational cost, since it avoids recourse to any eigenvalue analysis. It is noteworthy that the terms of this series correspond to the vibration modes of a simply supported beam, which coincides with the PRSI bridge model without any intermediate support. The orthogonality conditions for these terms, derived from (6) and (7) by posing, respectively, $c_{c,r} = k_{c,r} = 0$, for $r = 1, 2, \ldots, N_c$, are

$$\int_0^L m(x)\,\psi_i(x)\,\psi_j(x)\,dx = 0$$

$$\int_0^L b(x)\,\psi_i''(x)\,\psi_j''(x)\,dx = 0. \tag{26}$$

The application of these orthogonality conditions leads to a set of coupled Galerkin equations due to the nonzero terms $C_{c,ii}$ and $K_{c,ij}$ for $i \neq j$. These out of diagonal terms are discarded to obtain a diagonal problem.

6. Case Study

In this section, a realistic PRSI bridge [8] is considered as case study. First, the CMS method is applied to the bridge model by analyzing its modal properties and the related response to an impulsive input. Successively the seismic response is studied and a parametric analysis is carried out to investigate the influence of the intermediate support stiffness and damping on the seismic performance of the bridge components. Finally, the accuracy of the simplified analysis techniques is evaluated by comparing the results of the seismic analyses obtained with the CMS method and the RMS and FTS methods.

6.1. Case Study and Seismic Input Description. The PRSI bridge (Figure 2), whose properties are taken from [8], consists of a four-span continuous steel-concrete superstructure (span lengths $L_1 = 40$ m and $L_2 = 60$ m, for a total length $L = 200$ m) and of three isolated reinforced concrete piers. The value of the deck transverse stiffness is $EI_d = 1.1E + 09\,\text{kNm}^2$, which is an average over the values of EI_d that slightly vary along the bridge length due to the variation of the web and flange thickness. The deck mass per unit length is equal to $m_d = 16.24$ ton/m. The circular frequency corresponding to the first mode of vibration of the superstructure vibrating alone with no intermediate supports is $\omega_d = 2.03$ rad/s. The deck damping constant c_d is such that the first mode damping factor of the deck vibrating alone with no intermediate supports is equal to $\xi_d = 0.02$. The combined pier and isolator properties are described by Kelvin models, whose stiffness and damping constant are, respectively, $k_{c,2} = 2057.61$ kN/m and $c_{c,2} = 206.33$ kN/m for the central support and $k_{c1} = k_{c3} = 3500.62$ kN/m and $c_{c,1} = c_{c,3} = 322.69$ kN/m for the other supports. These support properties are the result of the design of isolation bearings ensuring the same shear demand at the base of the piers under the prefixed earthquake input.

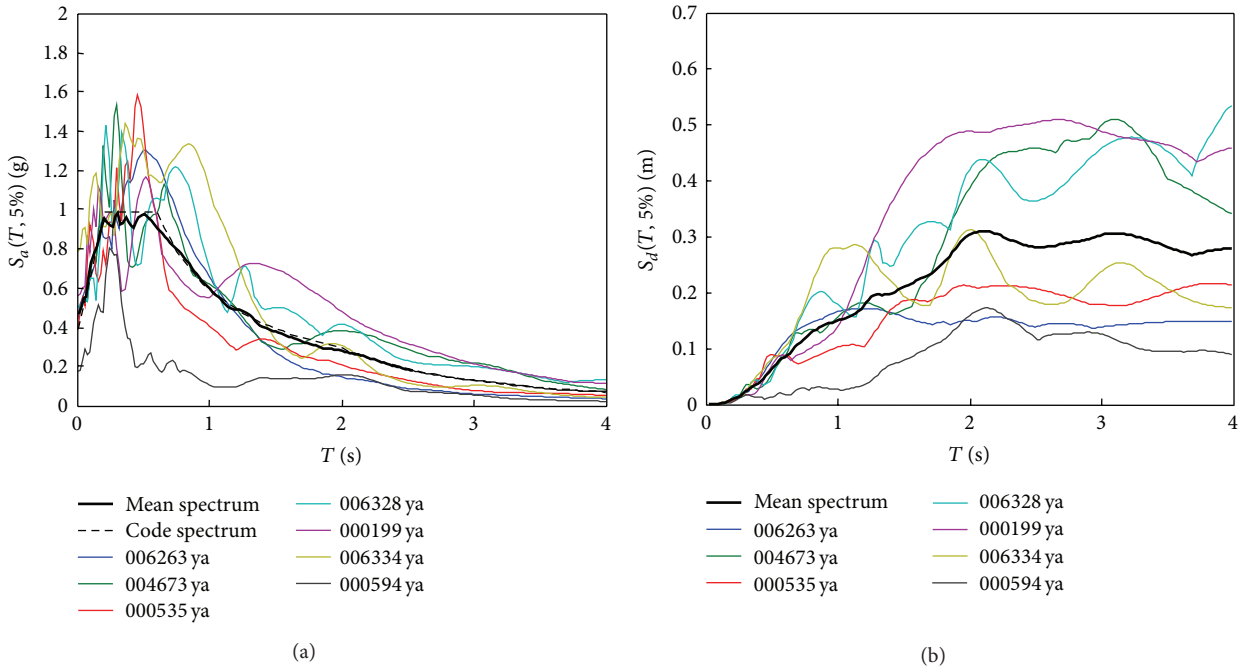

Figure 3: Variation with period T of the pseudo-acceleration response spectrum $S_a(T, 5\%)$ (a) and of the displacement response spectrum $S_d(T, 5\%)$ (b) of natural records.

Table 1: Modal properties: complex eigenvalues λ_i, undamped modal frequencies ω_{0i}, and damping ratios ξ_i.

Mode	λ_i [−]	ω_{0i} [rad/s]	ξ_i [−]
1	$-0.1723 - 2.6165i$	2.62	0.0657
2	$-0.2196 - 8.3574i$	8.36	0.0263
3	$-0.2834 - 18.4170i$	18.42	0.0154
4	$-0.1097 - 32.5180i$	32.52	0.0034
5	$-0.1042 - 50.7860i$	50.79	0.0021

The seismic input is described by a set of seven records compatible with the Eurocode 8-1 design spectrum, corresponding to a site with a peak ground acceleration (PGA) of $0.35Sg$ where S is the soil factor, assumed equal to 1.15 (ground type C), and g is the gravity acceleration. They have been selected from the European strong motion database [29] and fulfil the requirements of Eurocode 8 [30]. Figure 3(a) shows the pseudo-acceleration spectrum of the records, the mean spectrum, and the code spectrum, whereas Figure 3(b) shows the displacement response spectrum of the records and the corresponding mean spectrum.

6.2. Modal Properties and Impulsive Response. Table 1 reports the first 5 eigenvalues λ_i of the system, the corresponding vibration periods $T_{0i} = 2\pi/\omega_i$, and damping ratios ξ_i. These modal properties are determined by solving the eigenvalue problem corresponding to (5). It is noteworthy that the even modes of vibration are characterized by an antisymmetric shape and a participating factor equal to zero, and thus they do not affect the seismic response of the considered configurations (uniform support excitation is assumed).

In general, the effect of the intermediate restraints on the dynamic behaviour of the PRSI bridge is to increase the vibration frequency and damping ratio with respect to the case of the deck vibrating alone without any restraint. In fact, the fundamental vibration frequency shifts from the value $\omega_d = 2.03$ rad/s to $\omega_{01} = 2.62$ rad/s, corresponding to a first mode vibration period of about 2.40 s. The first mode damping ratio increases from $\xi_d = 0.02$ to $\xi_1 = 0.0657$. It should be observed that the value of ξ_1 is significantly lower than the value of the damping ratio of the internal and external intermediate viscoelastic supports at the same vibration frequency ω_{01}, equal to, respectively, 0.13 and 0.12. This is the result of the low dissipation capacity of the deck and of the dual load path behaviour of PRSI bridge, whose stiffness and damping capacity are the result of the contribution of both the deck and the intermediate supports [8, 9]. The damping ratio of the higher modes is in general very low and tends to decrease significantly with the increasing mode order.

Figure 4 shows the response of the midspan transverse displacement (Figure 4(a)) and of the abutment reactions (Figure 4(b)), for a unit impulse ground motion $\ddot{u}_g(t) = \delta(t)$. The analytical exact expression of the modal impulse response is reported in (16). The different response functions plotted in Figure 4 are obtained by considering (1) the contribution of the first mode only, (2) the contribution of the first and third modes, and (3) the contribution of the first, third, and fifth modes. Modes higher than the 5th have a negligible influence on the response. In fact, the mass participation factors of the 1st, 3rd, and 5th modes, evaluated through the RMS method, are 81%, 9.2%, and 3.25%. While the midspan displacement response is dominated by the first mode only, higher modes strongly affect the abutment

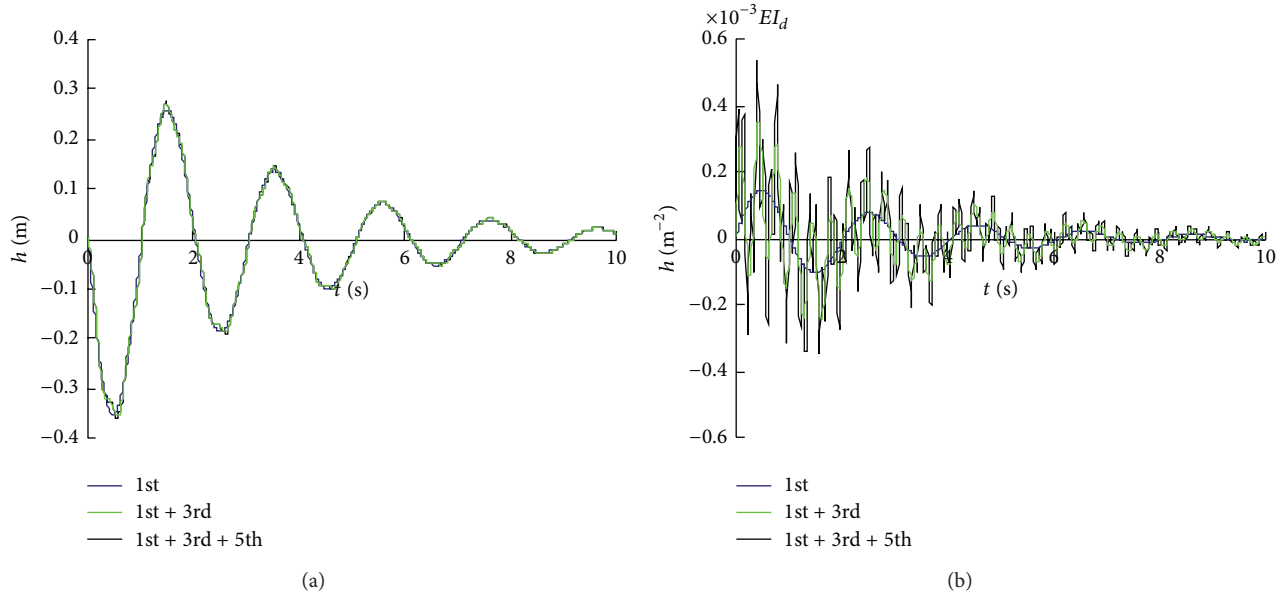

FIGURE 4: Response to impulsive loading (h) versus time (t) in terms of (a) midspan transverse displacement and (b) abutment reactions.

reactions. The impulse response in terms of the transverse bending moments, not reported here due to space constraints, is also influenced by the higher modes contribution, but at a less extent than the abutment reactions.

6.3. Seismic Response. In this section, the characteristic aspects of the seismic performance of PRSI bridges are highlighted by starting from the seismic analysis of the case study and by evaluating successively the response variations due to changes of the most important characteristic parameters of the bridge, that is, the deck-to-support stiffness ratio and the support damping. The bridge seismic performance is evaluated by monitoring the following response parameters: the midspan transverse displacement, the transverse bending moments, and the abutment shear. The CMS method is applied to compute the maximum overtime values of these response parameters by averaging the results obtained for the seven different records considered. Only the contribution of the first three symmetric vibration modes is considered due to the negligible influence of the other modes.

Figure 5 reports the mean of the envelopes of the transverse displacements and bending moments obtained for the different records. The displacement field coincides with a sinusoidal shape. This can be explained by observing that the isolated piers have a very low stiffness compared to the deck stiffness and, thus, their restraint action on the deck is negligible. Furthermore, the displacement response is in general dominated by the first mode of vibration. The transverse bending moments exhibit a different shape because they are significantly influenced by the higher modes of vibration. The support restraint action on the deck moments is almost negligible. It is noteworthy that differently from the case of fully isolated bridges, the bending moment demand in the deck may be very significant and attain the critical value corresponding to deck yielding, a condition that should be avoided according to EC8-2 [30].

In order to evaluate how the support stiffness and damping influence the seismic response of the bridge components, an extensive parametric study is carried out by considering a set of bridge models with the same superstructure, but with intermediate supports having different properties. Following [9], the intermediate supports properties can be synthetically described by the following nondimensional parameters:

$$\alpha^2 = \frac{\sum_{i=1}^{N_c} k_{c,i} \cdot L^3}{\pi^4 E I_d} = \frac{\sum_{i=1}^{N_c} k_{c,i}}{\omega_d^2 L m_d}$$
$$\gamma_c = \frac{\sum_{i=1}^{N_c} c_{c,i}}{2\alpha^2 \omega_d m_d L} = \frac{\sum_{i=1}^{N_c} c_{c,i}\omega_d}{2\sum_{i=1}^{N_c} k_{c,i}}. \quad (27)$$

The parameter α^2 denotes the relative support to deck stiffness. Low values of α^2 correspond to a stiff deck relative to the springs while high values correspond to a more flexible deck relative to the springs. Limit case $\alpha^2 = 0$ corresponds to the simply supported beam with no intermediate restraints. The parameter γ_c describes the energy dissipation of the supports and it is equal to the ratio between the energy dissipated by the dampers and the maximum strain energy in the springs, for a uniform transverse harmonic motion of the deck with frequency ω_d. These two parameters assume the values $\alpha^2 = 0.676$ and $\gamma_c = 0.095$ for the bridge considered previously.

In the following parametric study, the values of these parameters are varied by keeping the same distribution of stiffness and of damping of the original bridge, that is, by using the same scale factor for all the values of $k_{c,i}$ and the same scaling factor for all the values of $c_{c,i}$. In particular, the values of α^2 are assumed to vary in the range between 0 (no intermediate supports) and 2 (stiff supports relative to the superstructure), whereas the values of γ_c are assumed to

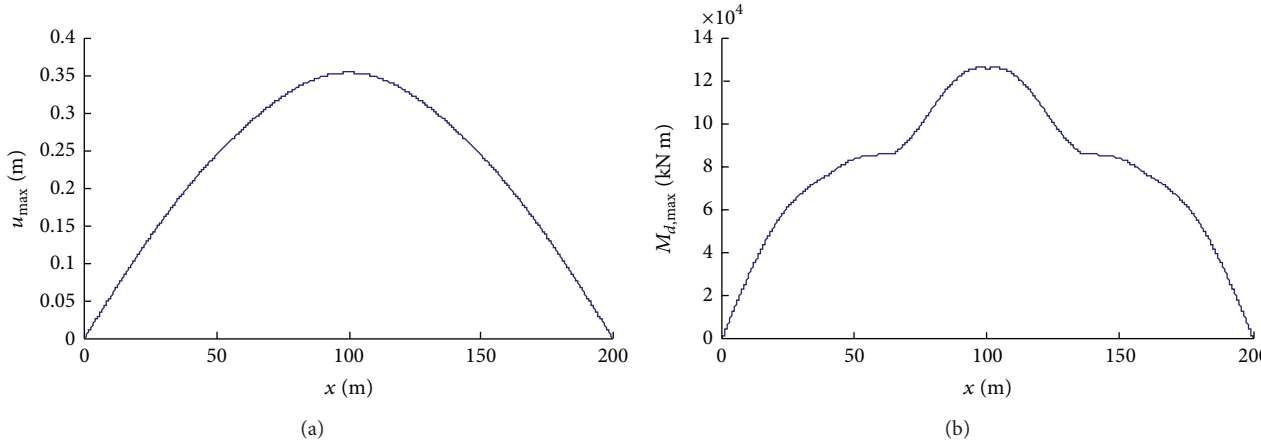

FIGURE 5: Average peak transverse displacements u_{max} (a) and bending moments $M_{d,max}$ (b) along the deck.

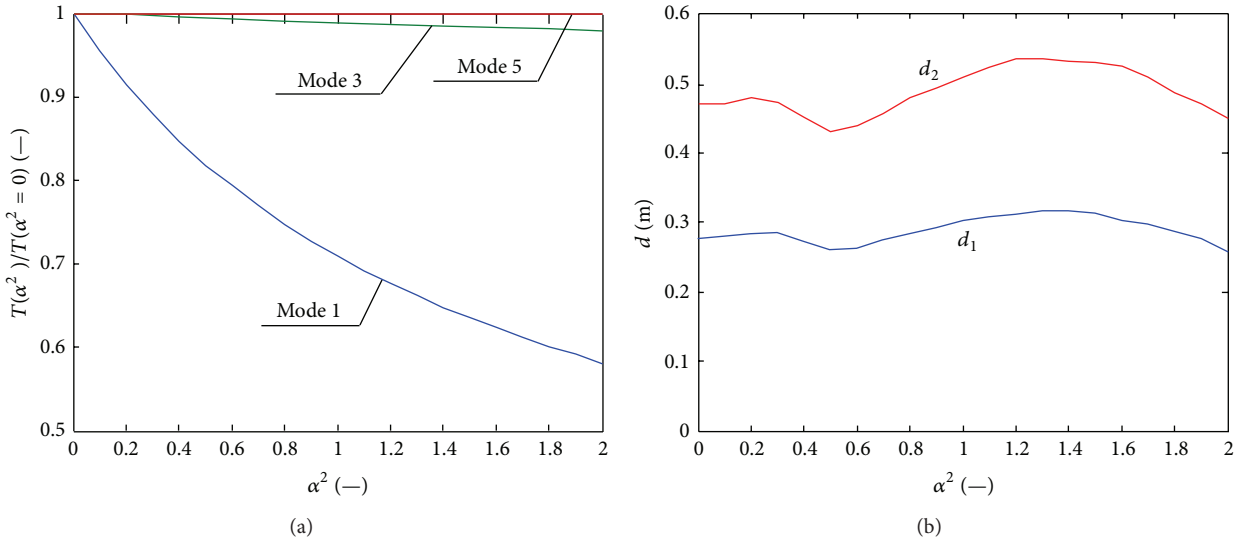

FIGURE 6: (a) Variation with α^2 of normalized transverse period $T(\alpha^2)/T(\alpha^2 = 0)$; (b) variation with α^2 of displacement demand of the deck in correspondence with the external piers (d_1) and the central pier (d_2).

vary in the range between 0 (intermediate supports with no dissipation capacity) and 0.3 (very high dissipation capacity).

Figure 6(a) shows the variation with α^2 of the periods of the first three modes of vibration that participate in the seismic response, that is, modes 1, 3, and 5, normalized with respect to the values observed for $\alpha^2 = 0$. It can be seen that only the fundamental vibration period is affected significantly by the support stiffness, whereas the higher modes of vibration exhibit a constant value of the vibration period for the different α^2 values. Figure 6(b) provides some information on the seismic response and it shows the influence of α^2 on the average maximum transverse displacements in correspondence with the outer intermediate supports and at the centre of the deck, denoted, respectively, as d_1 and d_2. These response quantities do not vary significantly with α^2. This occurs because the displacement demand is controlled by the first mode of vibration, whose period for the different α^2 values falls within the region corresponding to the flat displacement response spectrum.

Figure 7(a) shows the variation of the bending moment demand in correspondence with the piers, M_{d1}, and at the centre of the deck, M_{d2}. These response parameters follow a trend similar to that of the displacement demand; that is, they do not vary significantly with α^2. Figure 7(b) shows the variation with α^2 of the sum of the pier reaction forces (R_p) and the sum of the abutment reactions (R_{ab}). In the same figure, the contribution of the first mode only to these quantities ($R_{p,1}$, $R_{ab,1}$) is also reported. It can be observed that the total base shear of the system increases for increasing values of α^2, consistently with the increase of spectral acceleration at the fundamental vibration period. Furthermore, while the values of R_p tend to increase for increasing values of α^2, the values of R_{ab} remain almost constant. This can be explained by observing that the abutment reactions are significantly affected by the contribution of higher modes. Thus, in the case of intermediate support with no dissipation capacity, increasing the intermediate support stiffness does not reduce the shear forces transmitted to the abutments.

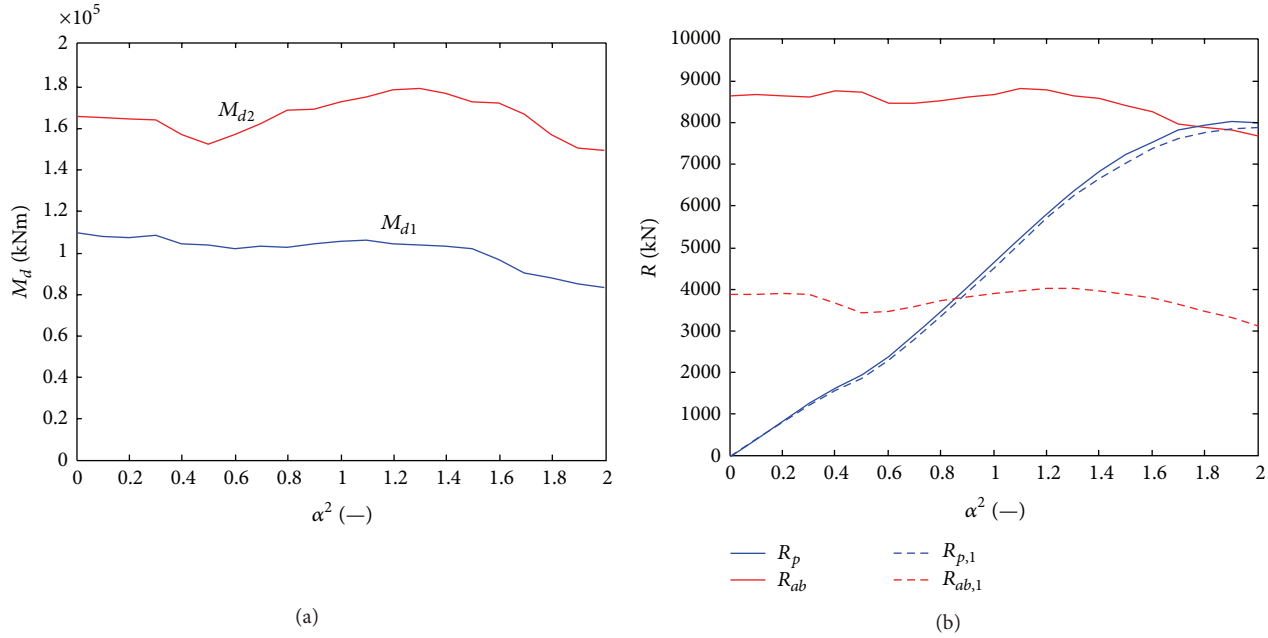

FIGURE 7: (a) Variation with α^2 of the peak average bending moments in correspondence with the external piers (M_{d1}) and the central pier (M_{d2}); (b) variation with α^2 of the peak average total pier reactions (R_p) and abutment reactions (R_{ab}) and of the corresponding first mode contribution ($R_{p,1}$, $R_{ab,1}$).

In the following, the joint influence of support stiffness and damping on the bridge seismic response is analysed. Figure 8(a) shows the variation of the transverse displacement d_2 versus α^2, for different values of γ_c. The values of d_2 are normalized, for each value of α^2, by dividing them by the value $d_{2,0}$ corresponding to $\gamma_c = 0$. As expected, the displacement demand decreases by increasing the dissipation capacity of the supports. Furthermore, the differences between the displacement demands for the different γ_c values reduce for α^2 tending to zero.

Figure 8(b) shows the total pier (R_p) and abutment (R_{ab}) shear demand versus α^2, for different values of γ_c. These values are normalized, for a given value of α^2, by dividing, respectively, by the values $R_{p,0}$ and $R_{ab,0}$ corresponding to $\gamma_c = 0$. It can be noted that both the pier and abutment reactions decrease by increasing γ_c. Furthermore, differently from the case corresponding to $\gamma_c = 0$, the increase of the intermediate support stiffness results in a reduction of the abutment reactions. However, the maximum decrease of the values of the abutment reactions, achieved for high α^2 levels, is inferior to the maximum decrease of the values of pier reactions. This is a consequence of the combined effects of (a) the contribution of higher modes, which is significant only for the abutment reactions and negligible for the pier reactions, and (b) the reduced efficiency of the intermediate dampers in damping the higher modes of vibration [9].

Finally, Figure 9 shows the total base shear versus α^2, for different values of γ_c. By increasing α^2, the total base shear increases for low support damping values ($\gamma_c = 0.0, 0.05$) while for very high γ_c values ($\gamma_c = 0.10, 0.15, 0.20$) it first decreases and then it slightly increases. Thus, for values of γ_c higher than 0.05, the total base shear is minimized when α^2 is equal to about 0.5. This result could be useful for the preliminary design of the isolator properties ensuring the minimization of the total base shear as performance objective.

6.4. Accuracy of Simplified Analysis Techniques. In this section, the accuracy of the simplified analysis techniques is evaluated by comparing the exact estimates of the response obtained by applying the CMS method with the corresponding estimates obtained by employing the RMS and FTS methods. In the application of all these methods, the first three symmetric terms of the set of approximating functions are considered and the ground motion records are those already employed in the previous section.

Figure 10 reports the results of the comparison for the case study described at the beginning of this section. It can be observed that the RMS and FTS method provide very close estimates of the mean transverse displacements (Figure 10(a)), whose shape is sinusoidal. This result was expected, since vibration modes higher than the first mode have a negligible influence on the displacements, as already pointed out in Figure 4. With reference to the transverse bending moment envelope (Figure 10(b)), the mean shape according to RMS and FTS agrees well with the exact shape, the highest difference being in correspondence with the intermediate restraints. The influence of the third mode of vibration on the bending moments shape is well described by both simplified techniques.

Table 2 reports and compares the peak values of the midspan displacement d_2, the transverse abutment reaction R_{ab}, the midspan transverse moments M_d, and the support

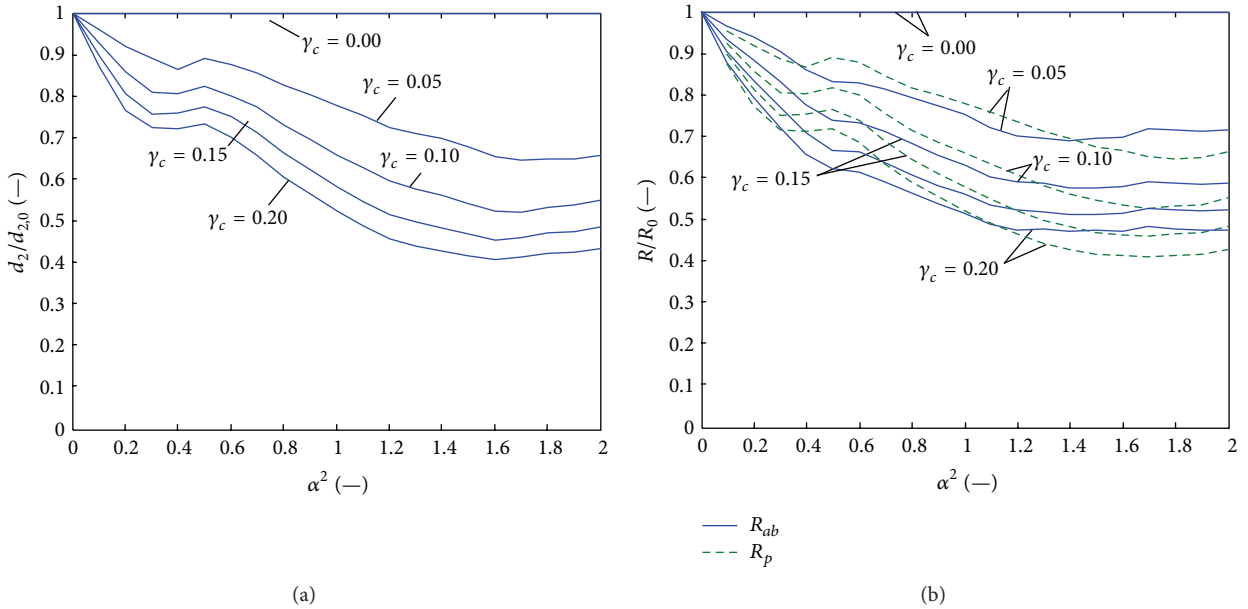

Figure 8: Variation with α^2 and for different values of γ_c of normalized deck centre transverse displacement $d_2/d_{2,0}$ and of the normalized total pier and abutment reactions ($R_p/R_{p,0}$ and $R_{ab}/R_{ab,0}$).

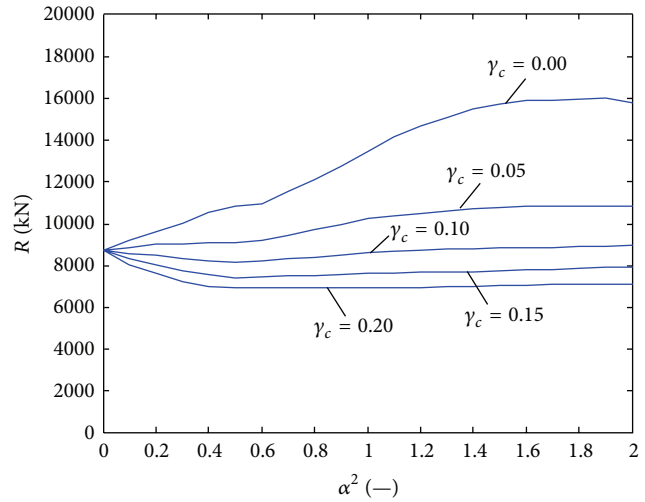

Figure 9: Variation with α^2 of total base shear R for different values of γ_c.

Table 2: Comparison of results according to the different analysis techniques for each of the 7 ground motion records considered.

Record	d_2 [m]			R_{ab} [kN]			M_d [MNm]			R_{p1} [kN]			R_{p2} [kN]		
	CMS	RMS	FTS	CMS	RMS	FTS	CMS	RMS	FTS	CMS	RMS	FTS	CMS	RMS	FTS
#1	0.1828	0.1827	0.1824	2105.6	2103.2	2119.8	71.788	71.779	72.022	369.8	370.2	372.3	376.1	376.0	375.2
#2	0.5496	0.5496	0.5485	4114.4	4093.8	4184.5	188.809	188.837	189.684	1126.5	1125.6	1131.3	1130.9	1130.9	1128.5
#3	0.2681	0.2681	0.2676	3320.5	3317.3	3315.7	103.350	103.412	103.921	520.8	519.9	523.0	551.6	551.7	550.6
#4	0.4473	0.4474	0.4468	3185.9	3180.3	3205.0	143.742	143.659	144.171	947.7	947.4	953.5	920.5	920.6	919.2
#5	0.6227	0.6227	0.6215	3650.2	3660.8	3782.8	194.330	194.336	195.329	1219.9	1220.2	1229.3	1281.3	1281.3	1278.8
#6	0.2417	0.2418	0.2416	3335.4	3328.3	3345.6	116.320	116.249	116.587	508.7	508.3	511.6	497.4	497.5	497.1
#7	0.1680	0.1680	0.1678	1648.8	1662.8	1683.0	65.313	65.334	65.723	336.3	335.8	338.1	345.6	345.7	345.3

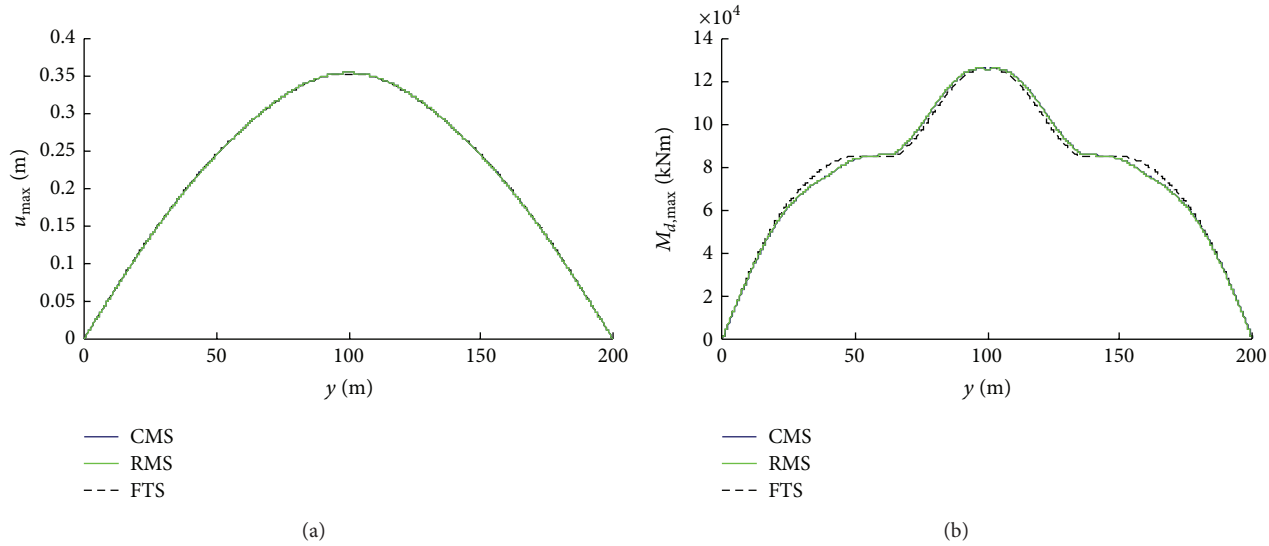

FIGURE 10: Transverse displacements u_{max} (a) and bending moments $M_{d,max}$ (b) along the deck according to the exact and the simplified analysis techniques.

TABLE 3: Comparison of results (mean values and CoV of the response) according to the different analysis techniques.

Response parameter	CMS		RMS		FTS	
	Mean	CoV	Mean	CoV	Mean	CoV
d_2 [m]	0.3543	0.519	0.3543	0.519	0.3537	0.519
R_{ab} [kN]	3051.55	0.284	3049.47	0.282	3090.92	0.287
M_d [kNm]	126235.75	0.411	126249.35	0.411	126778.66	0.411
R_{p1} [kN]	718.52	0.515	718.22	0.515	722.73	0.515
R_{p2} [kN]	729.05	0.519	729.09	0.519	727.83	0.519

reactions R_{p1} and R_{p2} according to the three analysis techniques, for the 7 records employed to describe the record-to-record variability effects. These records are characterized by different characteristics in terms of duration and frequency content (Figure 3). Thus, the values of the response parameters of interest exhibit significant variation from record to record. The level of accuracy of the simplified analysis techniques is in general very high and it is only slightly influenced by the record variability. The highest relative error, observed for the estimates of the bending moment demand, is about 0.84% for the RMS method and 3.6% for the FTS method. The coupling indexes for the damping matrix are $\alpha_{13} = 0.0454$, $\alpha_{15} = 0.2259$, and $\alpha_{35} = 0.1358$ for the RMS method and $\alpha_{13} = 0.0461$, $\alpha_{15} = 0.2242$, and $\alpha_{35} = 0.1365$ for the FTS method. The coupling indexes for the stiffness matrix are $\beta_{13} = 5.59e-4$, $\beta_{15} = 9.04e-5$, and $\beta_{35} = 1.83e-6$ for the FTS method. Thus, the extent of coupling in both the stiffness and damping terms is very low and this explains why the approximate techniques provide accurate response estimates.

Table 3 reports the mean value and coefficient of variation of the monitored response parameters. With reference to this application, it can be concluded that both the simplified analysis techniques provide very accurate estimates of the response statistics despite the approximations involved in their derivation. The highest relative error between the results of the simplified analysis techniques and those of the CMS method is observed for the estimates of the mean bending moment demand and it is about 0.01% for the RMS method and 0.43% for the FTS method.

The accuracy of the approximate techniques is also evaluated by considering another set of characteristic parameters, corresponding to $\alpha^2 = 2$ and $\gamma_c = 0.2$, and representing intermediate supports with high stiffness and dissipation capacity.

The displacement shape of the bridge, reported in Figure 11(a), is sinusoidal, despite the high stiffness and damping capacity of the supports. However, the bending moment shape, reported in Figure 11(b), is significantly influenced by the higher modes of vibration and by the restrain action of the supports. The RMS method provides very accurate estimates of this shape, whereas the FTS method is not able to describe the support restraint effect.

Table 4 reports the peak values of the response parameters of interest for each of the 7 natural records considered, according to the different analysis techniques. The highest relative error, observed for the estimates of the bending moment demand, is less than 3.6% for the RMS method and 9.2% for the FTS method.

The mean and coefficient of variation of the response parameters of interest are reported in Table 5. The highest relative error, with respect to the CMS estimate, is observed for the mean bending moment demand and it is less than

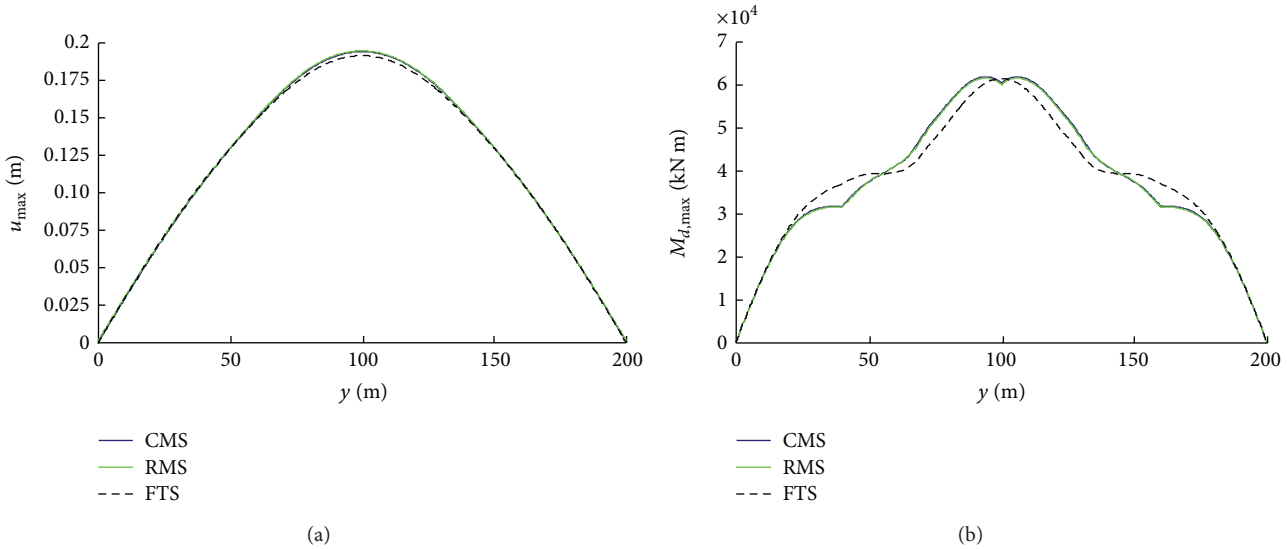

Figure 11: Transverse displacements u_{max} (a) and bending moments $M_{d,max}$ (b) along the deck according to the exact and the simplified analysis techniques.

Table 4: Comparison of results according to the different analysis techniques for each of the 7 ground motion records considered.

Record	d_2 [m]			R_{ab} [kN]			M_d [MNm]			R_{p1} [kN]			R_{p2} [kN]		
	CMS	RMS	FTS	CMS	RMS	FTS	CMS	RMS	FTS	CMS	RMS	FTS	CMS	RMS	FTS
#1	0.1556	0.1557	0.1548	1468.2	1512.9	1435.2	65.801	65.840	65.878	846.0	832.5	846.0	948.2	947.8	942.4
#2	0.2099	0.2096	0.2077	2114.9	2175.0	2175.6	74.322	73.745	72.942	1197.8	1187.6	1200.9	1279.6	1275.7	1264.2
#3	0.1504	0.1505	0.1490	1854.3	1871.9	1905.0	60.887	59.777	59.856	890.7	883.8	890.5	916.9	916.0	907.0
#4	0.2164	0.2167	0.2144	2169.8	2198.6	2198.9	78.089	78.244	77.744	1183.2	1171.2	1190.7	1319.0	1318.6	1305.0
#5	0.3471	0.3475	0.3439	2088.8	2016.8	2239.5	105.322	104.517	103.797	2107.2	2099.2	2128.0	2115.7	2114.8	2093.3
#6	0.1971	0.1966	0.1954	1948.0	1955.0	1783.2	83.645	82.237	82.389	1088.8	1102.9	1126.8	1201.4	1196.8	1189.1
#7	0.0799	0.0799	0.0790	968.2	958.5	932.9	30.202	29.984	30.055	464.0	459.4	464.6	486.8	486.3	480.6

Table 5: Comparison of results (mean values and CoV of the response) according to the different analysis techniques.

Response parameter	CMS		RMS		FTS	
	Mean	CoV	Mean	CoV	Mean	CoV
d_2 [m]	0.1938	0.425	0.1938	0.425	0.1920	0.424
R_{ab} [kN]	1801.7	0.243	1812.6	0.243	1810.0	0.266
M_d [kNm]	71181.2	0.324	70620.6	0.324	70380.0	0.322
R_{p1} [kN]	1111.1	0.456	1105.2	0.458	1121.1	0.458
R_{p2} [kN]	1181.1	0.425	1179.4	0.425	1168.8	0.424

0.79% for the RMS method and 1.12% for the FTS method. The coupling indexes for the damping matrix are $\alpha_{13} = 0.0625$, $\alpha_{15} = 0.4244$, and $\alpha_{35} = 0.2266$ for the RMS method and $\alpha_{13} = 0.0652$, $\alpha_{15} = 0.4151$, and $\alpha_{35} = 0.2305$ for the FTS method. The coupling indexes for the stiffness matrix are $\beta_{13} = 0.0027$, $\beta_{15} = 4.43e-4$, and $\beta_{35} = 1.56e-5$. In general, these coefficients assume higher values compared to the values observed in the other bridge (Tables 2 and 4). In any case, the dispersion of the response due to the uncertainties in the values of the parameters describing the pier and the bearings might be more important than the error due to the use of simplified analysis methods.

7. Conclusions

This paper proposes a formulation and different analysis technique for the seismic assessment of partially restrained seismically isolated (PRSI) bridges. The formulation is based on a description of the bridges by means of a simply supported continuous beam resting on intermediate viscoelastic supports, whose properties are calibrated to represent the pier/bearing systems. The first analysis technique developed in this paper is based on the complex modes superposition (CMS) method and provides an exact solution to the seismic problem by accounting for nonclassical damping. This technique can be employed to evaluate the influence of

the complex vibration modes on the response of the bridge components and also provides a reference solution against which simplified analysis approaches can be tested. The other two proposed techniques are based on the assumed modes method and on a simplified description of the damping properties. The real mode superposition (RMS) method employs a series expansion of the displacement field in terms of the classic modes of vibration, whereas the Fourier terms superposition (FTS) method employs a series expansion based on the Fourier sine-only series terms.

A realistic PRSI bridge model is considered and its seismic response under a set of ground motion records is analyzed by employing the CMS method. This method reveals that the bridge components are differently affected by higher modes of vibration. In particular, while the displacement demand is mainly influenced by the first mode, other parameters such as the bending moments and abutment reactions are significantly affected by the contribution of higher modes. A parametric study is then carried out to evaluate the influence of intermediate support stiffness and damping on the seismic response of the main components of the PRSI bridge. These support properties are controlled by two nondimensional parameters whose values are varied in the parametric analysis. Based on the results of the study, it can be concluded that (1) in the case of intermediate support with low damping capacity, the abutment reactions do not decrease significantly by increasing the support stiffness; (2) increasing the support damping results in a decrease in the abutment reactions which is less significant than the decrease in the pier reactions; (3) for moderate to high dissipation capacity of the intermediate supports, there exists an optimal value of the damping that minimizes the total shear transmitted to the foundations.

Finally, the accuracy of the simplified analyses techniques is evaluated by comparing the results of the seismic analyses carried out by employing the CMS method with the corresponding results obtained by employing the two simplified techniques. Based on the results presented in this paper, it is concluded that, for the class of bridges analyzed, (1) the extent of nonclassical damping is usually limited and (2) satisfactory estimates of the seismic response are obtained by considering the simplified analysis approaches.

Appendix

The analytical solution of the eigenvalue problem is obtained under the assumption that $m(x)$, $b(x)$, and $c(x)$ are constant along the beam length and equal, respectively, to m_d, EI_d, and c_d. The beam is divided into a set of N_s segments, each bounded by two consecutive restraints (external or intermediate). The function $u_s(z_s, t)$ describing the motion of the sth segment of length L_s is decomposed into the product of a spatial function $\psi_s(z_s)$ and of a time-dependent function $Z(t) = Z_0 e^{\lambda t}$. The function $\psi_s(z_s)$ must satisfy the following equation:

$$\psi_s^{IV}(z_s, t) = \Omega^4 \psi_s(z_s, t), \tag{A.1}$$

where $\Omega^4 = -(\lambda^2 m_d + \lambda c_d)/EI_d$.

The solution to (A.1) can be expressed as

$$\begin{aligned}\psi_s(z_s) = {} & C_{4s-3}\sin(\Omega z_s) + C_{4s-2}\cos(\Omega z_s) \\ & + C_{4s-1}\sinh(\Omega z_s) + C_{4s}\cosh(\Omega z_s)\end{aligned} \tag{A.2}$$

with C_{4s-3}, C_{4s-2}, C_{4s-1}, and C_{4s} to be determined based on the boundary conditions at the external supports and the continuity conditions at the intermediate restraints. This involves the calculation of higher order derivatives up to the third order.

In total, a set of $4N_s$ conditions is required to determine the vibration shape along the whole beam. At the first span the conditions $\psi_1(0) = \psi_1''(0) = 0$ apply while at the last span the support conditions are $\psi_{N_s}(L_{N_s}) = \psi_{N_s}''(L_{N_s}) = 0$. The boundary conditions at the intermediate spring locations are

$$\begin{aligned}\psi_{s-1}(L_{s-1}) &= \psi_s(0) \\ \psi_{s-1}'(L_{s-1}) &= \psi_s'(0) \\ \psi_{s-1}''(L_{s-1}) &= \psi_s''(0) \\ EI_d\left[\psi_{s-1}'''(L_{s-1}) - \psi_s'''(0)\right] &- (k_{c,s} + \lambda c_{c,s})\psi_s(0) = 0.\end{aligned} \tag{A.3}$$

By substituting (A.2) into the boundary (supports and continuity) conditions, a system of $4N_s$ homogeneous equations in the constants $C_1, \ldots, C_{4N_s}$ is obtained. Since the system is homogeneous, the determinant of coefficients must be equal to zero for the existence of a nontrivial solution. This procedure yields the following frequency equation in the unknown λ:

$$\begin{aligned}G\left(m_d, EI_d, c_d, L_1, \ldots, L_{N_s}, k_{c,1}, \ldots, k_{c,N_c}, c_{c,1}, \ldots, c_{c,N_c}, \lambda\right) \\ = 0.\end{aligned} \tag{A.4}$$

In the general case of nonzero damping, the solution of the equation must be sought in the complex domain. It is noteworthy that, since the system is continuous, an infinite set of eigenvalues λ are obtained which satisfy (A.4). However, only selected values of λ are significant, because they correspond to the first vibration modes which are usually characterized by the highest participation factors. It is also noteworthy that the eigensolutions appear in complex pairs. Thus, if λ_i satisfies (A.4), then also its complex conjugate $\overline{\lambda}_i$ satisfies (A.4). The eigenvectors corresponding to these eigenvalues are complex conjugate, too. Finally, it is observed that the undamped circular vibration frequency ω_i and damping ratio ξ_i corresponding to the ith mode can be obtained by recalling that $\lambda_i\overline{\lambda}_i = {\omega_i}^2$ and $\lambda_i + \overline{\lambda}_i = -2\xi_i\omega_i$. For zero damping, $\lambda = i\omega$ and the vibration modes are real.

Conflict of Interests

The authors declare that there is no conflict of interests regarding the publication of this paper.

Acknowledgment

The reported research was supported by the Italian Department of Civil Protection within the Reluis-DPC Projects 2014. The authors gratefully acknowledge this financial support.

References

[1] M. T. A. Chaudhary, M. Abé, and Y. Fujino, "Performance evaluation of base-isolated Yama-agé bridge with high damping rubber bearings using recorded seismic data," *Engineering Structures*, vol. 23, no. 8, pp. 902–910, 2001.

[2] G. C. Lee, Y. Kitane, and I. G. Buckle, "Literature review of the observed performance of seismically isolated bridges," Research Progress and Accomplishments: 2000–2001, MCEER, State University of New York, Buffalo, NY, USA, 2001.

[3] R. L. Boroschek, M. O. Moroni, and M. Sarrazin, "Dynamic characteristics of a long span seismic isolated bridge," *Engineering Structures*, vol. 25, no. 12, pp. 1479–1490, 2003.

[4] J. Shen, M. H. Tsai, K. C. Chang, and G. C. Lee, "Performance of a seismically isolated bridge under near-fault earthquake ground motions," *Journal of Structural Engineering*, vol. 130, no. 6, pp. 861–868, 2004.

[5] K. L. Ryan and W. Hu, "Effectiveness of partial isolation of bridges for improving column performance," in *Proceedings of the Structures Congress*, pp. 1–10, 2009.

[6] M.-H. Tsai, "Transverse earthquake response analysis of a seismically isolated regular bridge with partial restraint," *Engineering Structures*, vol. 30, no. 2, pp. 393–403, 2008.

[7] N. Makris, G. Kampas, and D. Angelopoulou, "The eigenvalues of isolated bridges with transverse restraints at the end abutments," *Earthquake Engineering and Structural Dynamics*, vol. 39, no. 8, pp. 869–886, 2010.

[8] E. Tubaldi and A. Dall'Asta, "A design method for seismically isolated bridges with abutment restraint," *Engineering Structures*, vol. 33, no. 3, pp. 786–795, 2011.

[9] E. Tubaldi and A. Dall'Asta, "Transverse free vibrations of continuous bridges with abutment restraint," *Earthquake Engineering and Structural Dynamics*, vol. 41, no. 9, pp. 1319–1340, 2012.

[10] G. Della Corte, R. de Risi, and L. di Sarno, "Approximate method for transverse response analysis of partially isolated bridges," *Journal of Bridge Engineering*, vol. 18, no. 11, pp. 1121–1130, 2013.

[11] M. N. Fardis and G. Tsionis, "Eigenvalues and modes of distributed-mass symmetric multispan bridges with restrained ends for seismic response analysis," *Engineering Structures*, vol. 51, pp. 141–149, 2013.

[12] A. S. Veletsos and C. E. Ventura, "Modal analysis of nonclassically damped linear systems," *Earthquake Engineering & Structural Dynamics*, vol. 14, no. 2, pp. 217–243, 1986.

[13] A. M. Claret and F. Venancio-Filho, "Modal superposition pseudo-force method for dynamic analysis of structural systems with non-proportional damping," *Earthquake Engineering and Structural Dynamics*, vol. 20, no. 4, pp. 303–315, 1991.

[14] F. Venancio-Filho, Y. K. Wang, F. B. Lin, A. M. Claret, and W. G. Ferreira, "Dynamic analysis of nonproportional damping structural systems time and frequency domain methods," in *Proceedings of the 16th International Conference on Structural Mechanics in Reactor Technology (SMIRT '01)*, Washington, DC, USA, 2001.

[15] S. Kim, "On the evaluation of coupling effect in nonclassically damped linear systems," *Journal of Mechanical Science and Technology*, vol. 9, no. 3, pp. 336–343, 1995.

[16] G. Prater Jr. and R. Singh, "Quantification of the extent of nonproportional viscous damping in discrete vibratory systems," *Journal of Sound and Vibration*, vol. 104, no. 1, pp. 109–125, 1986.

[17] M. Morzfeld, F. Ma, and N. Ajavakom, "On the decoupling approximation in damped linear systems," *Journal of Vibration and Control*, vol. 14, no. 12, pp. 1869–1884, 2008.

[18] J. S. Hwang, K. C. Chang, and M. H. Tsai, "Composite damping ratio of seismically isolated regular bridges," *Engineering Structures*, vol. 19, no. 1, pp. 55–62, 1997.

[19] S. C. Lee, M. Q. Feng, S.-J. Kwon, and S.-H. Hong, "Equivalent modal damping of short-span bridges subjected to strong motion," *Journal of Bridge Engineering*, vol. 16, no. 2, pp. 316–323, 2011.

[20] P. Franchin, G. Monti, and P. E. Pinto, "On the accuracy of simplified methods for the analysis of isolated bridges," *Earthquake Engineering and Structural Dynamics*, vol. 30, no. 3, pp. 380–382, 2001.

[21] K. A. Foss, "Coordinates which uncouple the equations of motion of damped linear dynamic systems," *Journal of Applied Mechanics*, vol. 25, no. 3, pp. 361–364, 1958.

[22] G. Oliveto, A. Santini, and E. Tripodi, "Complex modal analysis of a flexural vibrating beam with viscous end conditions," *Journal of Sound and Vibration*, vol. 200, no. 3, pp. 327–345, 1997.

[23] M. Gürgöze and H. Erol, "Dynamic response of a viscously damped cantilever with a viscous end condition," *Journal of Sound and Vibration*, vol. 298, no. 1-2, pp. 132–153, 2006.

[24] E. Tubaldi, "Dynamic behavior of adjacent buildings connected by linear viscous/viscoelastic dampers," *Structural Control and Health Monitoring*, 2015.

[25] C. Truesdell and R. A. Toupin, "The classical field theories," in *Handbuch der Physik, Band III/l*, Springer, Berlin, Germany, 1960.

[26] G. Prater Jr. and R. Singh, "Eigenproblem formulation, solution and interpretation for nonproportionally damped continuous beams," *Journal of Sound and Vibration*, vol. 143, no. 1, pp. 125–142, 1990.

[27] M. N. Hamdan and B. A. Jubran, "Free and forced vibrations of a restrained uniform beam carrying an intermediate lumped mass and a rotary inertia," *Journal of Sound and Vibration*, vol. 150, no. 2, pp. 203–216, 1991.

[28] P. A. Hassanpour, E. Esmailzadeh, W. L. Cleghorn, and J. K. Mills, "Generalized orthogonality condition for beams with intermediate lumped masses subjected to axial force," *Journal of Vibration and Control*, vol. 16, no. 5, pp. 665–683, 2010.

[29] N. Ambraseys, P. Smith, R. Bernardi, D. Rinaldis, F. Cotton, and C. Berge-Thierry, *Dissemination of European Strong-Motion Data*, CD-ROM Collection, European Council, Environment and Climate Research Programme, 2000.

[30] European Committee for Standardization (ECS), "Eurocode 8—design of structures for earthquake resistance," EN 1998, European Committee for Standardization, Brussels, Belgium, 2005.